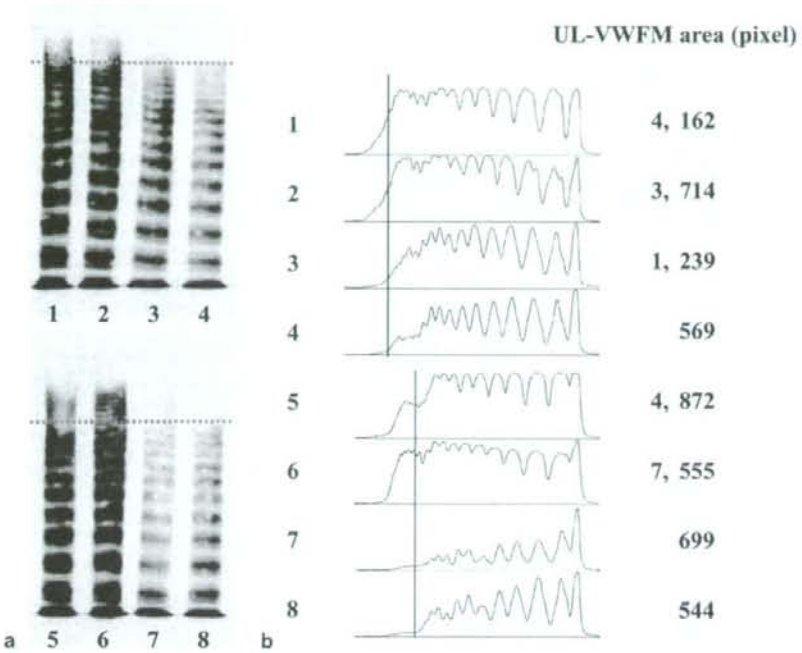

Fig. 3a,b. von Willebrand factor (VWF) multimeric analysis in two representative patients and its densitometric analysis. *1*, patient 1 before PCI in acute phase of AMI; *2*, after PCI of patient 1; *3*, chronic phase of patients 1; *4* and *8*, normal plasma; *5*, before PCI of patient 2; *6*, after PCI of patient 2; *7*, chronic phase of patient 2. **a** von Willebrand factor multimeric analysis was performed using 1% agarose gel electrophoresis. **b** Densitometric analyses of unusually large VWF multimer (*UL-VWFM*) using NIH image J (developed by the National Institute of Health, http://rsb.info.nih.gov/nih-image/). UL-VWF multimer was detected in samples obtained from the femoral vein before and after PCI in all AMI patients tested, though it was not detected in samples collected during the chronic phase

controls (3.3 ± 1.4), though there was no significant difference in the ratio among sampling points (Fig. 2c). In the chronic phase, those ratios decreased to levels similar to those seen in age-matched controls (FV, 3.2 ± 1.9; Ao, 3.0 ± 1.6; Cs, 3.0 ± 1.5) (Fig. 2c).

Detection of UL-VWFM

We analyzed UL-VWFM in 6 out of 26 AMI patients. UL-VWFM was detected in samples obtained from the FV before and after PCI in all patients (Fig 3a). It was not detected in samples collected during the chronic phase (Fig. 3a). To more easily quantify UL-VWFM levels, we performed densitometric analysis (Fig. 3b).

Circadian variation in plasma VWF:Ag and ADAMTS13 activity

Von Willebrand factor antigen was significantly higher in the morning (100% ± 42%) than in the evening (89% ± 41%) (Fig. 4a); however, for ADAMTS13 activity there was no significant difference between the morning (55% ± 13%) and the evening (61% ± 18%) (Fig. 4b). The ratio of VWF:Ag to ADAMTS13 activity was significantly higher at 09:30 (1.9 ± 0.8) than at 20:00 (1.5 ± 0.8) ($P < 0.05$, Fig. 4c).

Discussion

In the present study we simultaneously measured the activity of ADAMTS13 and the levels of its substrates (VWF:Ag and UL-VWFM) in plasma samples obtained from the FV, Ao, and Cs during the acute and chronic phases of AMI. We demonstrate for the first time that during the acute phase, the ratio of VWF:Ag to ADAMTS13 activity in AMI patients was significantly higher at all three sampling sites than in the peripheral blood of age-matched controls and that during the chronic phase of AMI, these ratios had returned to levels similar to those seen in age-matched controls. Moreover, UL-VWFM was detected during the acute phase but not in the chronic phase of AMI, in agreement with recent reports by Sakai et al.[6] and Goto et al.[12] In agreement with our findings, Kaikita et al.[13] also reported that the ratio of VWF:Ag to ADAMTS13 activity in peripheral venous plasma is higher in AMI patients than in those with stable exertional angina and chest pain syndrome.

During the last decade, evidence has accumulated that release of VWF:Ag from endothelial cells and platelets is a key early step toward occlusive thrombus formation in the coronary circulation. With that in mind, before the beginning of the present study we hypothesized that VWF:Ag would be much higher in the Cs than in the Ao or FV, and that ADAMTS13 activity might be lower in the Cs than in the FV or Ao. However, our study showed that there was

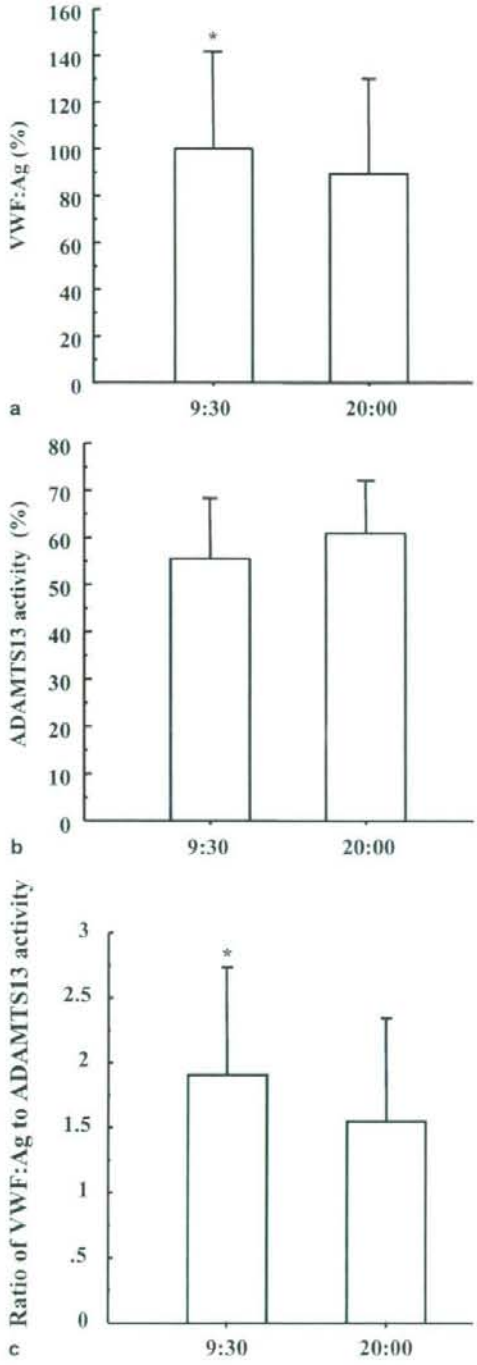

Fig. 4a–c. Comparison with von Willebrand factor antigen (*VWF:Ag*), ADAMTS13, and the ratio of VWF:Ag to ADAMTS13 activity between in the morning and in the evening. **a** VWF:Ag was significantly higher in the morning (100% ± 42%) than in the evening (89% ± 41%). **b** ADAMTS13 activity was no significant difference between in the morning (55% ± 13%) and the evening (61% ± 18%). **c** The ratio of VWF:Ag to ADAMTS13 activity was significantly higher at 09:30 than at 20:00. Shown are mean ± SD. $*P < 0.05$ vs 20:00

no significant difference in the plasma level of VWF:Ag, ADAMTS activity, and the ratio of VWF:Ag to ADAMTS13 activity among three sampling points, clearly indicating that AMI is not a local but rather a systemic prothrombotic condition. In other words, the present findings support the recent concept that occlusive coronary thrombi develop in vulnerable blood (prone to thrombosis) or in vulnerable patients.[14,15] Further studies are necessary to clarify whether increased VWF may lead to the formation of coronary thrombi or whether coronary thrombi itself may cause elevation of VWF levels in AMI.

It was previously reported that AMI frequently occurs in the morning, between 06:00 and 12:00, a vulnerable period for cardiovascular events,[16] and also frequently occurs after physical exercise, especially in the sun during summer. In that regard, we observed that the ratio of VWF:Ag to ADAMTS13 activity was higher in the morning than in the evening. Acute myocardial infarction is also more frequently observed in aged men than in young men. We previously reported that plasma ADAMTS13 activity declines and plasma VWF:Ag levels increase with increasing age, and that detectable levels of UL-VWFM were circulating in some older people.[11] Here, we confirmed that plasma VWF:Ag is 50% higher while plasma ADAMTS13 activity is nearly 50% lower in healthy age-matched control subjects as compared to young healthy subjects, resulting in a three-fold higher ratio of VWF:Ag to ADAMTS13 activity in the former than in the latter. Interestingly, we have also observed that physical exercise increases the ratio of VWF:Ag to ADAMTS13 activity in healthy men.[17] Thus the simultaneous measurement of ADAMTS13 activity and its substrate, VWF:Ag level, is useful in understanding the pathology of thrombotic diseases.

Although it is not possible to identify the precise site of production of VWF and ADAMTS13, our findings (together with those of others[5,6]) suggest that, during the acute phase of AMI, production of VWF is increased not only in coronary arterial endothelial cells and/or locally activated platelets, but also in systemic vascular beds and/or circulating endothelial cells. ADAMTS13 is mainly produced in hepatic stellate cells,[18] and is also synthesized in both human endothelial cells[19] and platelets,[20] suggesting that this enzyme is produced in the systemic circulation as well as in the liver.

In summary, we observed increased plasma VWF:Ag levels and relatively decreased ADAMTS13 activity in both systemic and coronary circulation during the acute phase of AMI, suggesting that an imbalance between the enzyme and its substrate may play an important predictive role in the formation of occlusive thrombi in a coronary

artery, ultimately leading to AMI. Further analysis of the production–consumption relation between VWF and ADAMTS13 in the coronary and systemic circulations will be necessary to understand the pathophysiological significance of VWF and ADAMTS13 in the formation of occlusive thrombi.

Acknowledgments This work was supported in part by research grants from the Ministry of Education, Culture, Sports, Science and Technology (to S.U., M.M., M.U., and Y.S.) and the Ministry of Health, Labour and Welfare (to M.M., Y.F., and Y.S.) of Japan.

References

1. Hoshiba Y, Hatakeyama K, Tanabe T, Goto S (2006) Co-localization of von Willebrand factor with platelet thrombi, tissue factor and platelets with fibrin, and consistent presence of inflammatory cells in coronary thrombi obtained by an aspiration device from patients with acute myocardial infarction. J Thromb Haemost 4:114–120
2. Mandelkorn JB, Wolf NM, Singh S, Shechter JA, Kersh RI, Rodgers DM, Workman MB, Bentivoglio LG, LaPorte SM, Meister SG (1983) Intracoronary thrombus in nontransmural myocardial infarction and in unstable angina pectoris. Am J Cardiol 52:1–6
3. Murasaki K, Kawana M, Murasaki S, Tsurumi Y, Tanoue K, Hagiwara N, Kasanuki H (2007) High P-selectin expression and low CD36 occupancy on circulating platelets are strong predictors of restenosis after coronary stenting in patients with coronary artery disease. Heart Vessels 22:229–236
4. Ruggeri ZM (1997) von Willebrand factor. J Clin Invest 100: S41–S46
5. Eto K, Isshiki T, Yamamoto H, Takeshita S, Ochiai M, Yokoyama N, Yoshimoto R, Ikeda Y, Sato T (1999) AJvW-2, an anti-vWF monoclonal antibody, inhibits enhanced platelet aggregation induced by high shear stress in platelet-rich plasma from patients with acute coronary syndrome. Arterioscler Thromb Vasc Biol 19:877–882
6. Sakai H, Goto S, Kim JY, Aoki N, Abe S, Ichikawa N, Yoshida M, Nagaoka Y, Handa S (2000) Plasma concentration of von Willebrand factor in acute myocardial infarction. Thromb Haemost 84:204–209
7. Jansson JH, Nilsson TK, Johnson O (1991) von Willebrand factor in plasma: a novel risk factor for recurrent myocardial infarction and death. Br Heart J 66:351–355
8. Folsom AR, Wu KK, Rosamond WD, Sharrett AR, Chambless LE (1997) Prospective study of hemostatic factors and incidence of coronary heart disease. Circulation 96:1102–1108
9. Fujimura Y, Matsumoto M, Yagi H, Yoshioka A, Matsui T, Titani K (2002) von Willebrand factor-cleaving protease and Upshaw-Schulman syndrome. Int J Hematol 75:25–34
10. Kato S, Matsumoto M, Matsuyama T, Isonishi A, Hiura H, Fujimura Y (2006) Novel monoclonal antibody-based enzyme immunoassay for determining plasma levels of ADAMTS13 activity. Transfusion 46:1444–1452
11. Matsumoto M, Kawaguchi S, Ishizashi H, Yagi H, Iida J, Sakaki T, Fujimura Y (2005) Platelets treated with ticlopidine are less reactive to unusually large von Willebrand factor multimers than are those treated with aspirin under high shear stress. Pathophysiol Haemost Thromb 34:35–40
12. Goto S, Sakai H, Goto M, Ono M, Ikeda Y, Handa S, Ruggeri ZM (1999) Enhanced shear-induced platelet aggregation in acute myocardial infarction. Circulation 99:608–613
13. Kaikita K, Soejima K, Matsukawa M, Nakagaki T, Ogawa H (2006) Reduced von Willebrand factor-cleaving protease (ADAMTS13) activity in acute myocardial infarction. J Thromb Haemost 4: 2490–2493
14. Naghavi M, Libby P, Falk E, Casscells SW, Litovsky S, Rumberger J, Badimon JJ, Stefanadis C, Moreno P, Pasterkamp G, Fayad Z, Stone PH, Waxman S, Raggi P, Madjid M, Zarrabi A, Burke A, Yuan C, Fitzgerald PJ, Siscovick DS, de Korte CL, Aikawa M, Airaksinen KE, Assmann G, Becker CR, Chesebro JH, Farb A, Galis ZS, Jackson C, Jang IK, Koenig W, Lodder RA, March K, Demirovic J, Navab M, Priori SG, Rekhter MD, Bahr R, Grundy SM, Mehran R, Colombo A, Boerwinkle E, Ballantyne C, Insull W Jr, Schwartz RS, Vogel R, Serruys PW, Hansson GK, Faxon DP, Kaul S, Drexler H, Greenland P, Muller JE, Virmani R, Ridker PM, Zipes DP, Shah PK, Willerson JT (2003) From vulnerable plaque to vulnerable patient: a call for new definitions and risk assessment strategies: Part II. Circulation 108:1772–1778
15. Goto S (2004) Propagation of arterial thrombi: local and remote contributory factors. Arterioscler Thromb Vasc Biol 24:2207–2208
16. Muller JE, Stone PH, Turi ZG, Rutherford JD, Czeisler CA, Parker C, Poole WK, Passamani E, Roberts R, Robertson T (1985) Circadian variation in the frequency of onset of acute myocardial infarction. N Engl J Med 313:1315–1322
17. Claus RA, Bockmeyer CL, Sossdorf M, Losche W, Hilberg T (2006) Physical stress as a model to study variations in ADAMTS-13 activity, von Willebrand factor level and platelet activation. J Thromb Haemost 4:902–905
18. Uemura M, Tatsumi K, Matsumoto M, Fujimoto M, Matsuyama T, Ishikawa M, Iwamoto T, Mori T, Wanaka A, Fukui H, Fujimura Y (2005) Localization of ADAMTS13 to the stellate cells of human liver. Blood 106:922–924
19. Turner N, Nolasco L, Tao Z, Dong JF, Moake J (2006) Human endothelial cells synthesize and release ADAMTS-13. J Thromb Haemost 4:1396–1404
20. Suzuki M, Murata M, Matsubara Y, Uchida T, Ishihara H, Shibano T, Ashida S, Soejima K, Okada Y, Ikeda Y (2004) Detection of von Willebrand factor-cleaving protease (ADAMTS13) in human platelets. Biochem Biophys Res Commun 313:212–216

Nephrol Dial Transplant (2008) 23: 3152–3159
doi: 10.1093/ndt/gfn240
Advance Access publication 7 May 2008

Original Article

NDT
Nephrology Dialysis Transplantation

Prediction of corticosteroid responsiveness based on fibroblast-specific protein 1 (FSP1) in patients with IgA nephropathy

Koji Harada, Yasuhiro Akai, Yukinari Yamaguchi, Kuniko Kimura, Yoshiharu Nishitani, Kimihiko Nakatani, Masayuki Iwano and Yoshihiko Saito

1st Department of Internal Medicine, Nara Medical University, Kashihara, Nara, Japan

Abstract

Background. Corticosteroids are frequently used to treat patients with active IgA nephropathy (IgAN); however, there have been few reports describing factors that are predictive of the response to corticosteroid treatment. The purpose of this study is to determine the extent to which fibroblast-specific protein 1-positive ($FSP1^+$) cells are predictive of corticosteroid responsiveness in patients with IgAN.

Methods. Fifty biopsy-proven IgAN patients who received corticosteroid therapy were enrolled and followed for 7.1 ± 3.0 years. $FSP1^+$ cells were identified using an anti-FSP1 antibody.

Results. Twelve patients showed progression of renal impairment or no reduction of urinary protein (non-responders) after steroid therapy. In the remaining 38 patients, renal function was stable during follow-up, and their urinary protein declined to <1.0 g/day (responders). Serum creatinine, estimated GFR, severity of mesangial proliferation, percent glomerulosclerosis/total glomeruli, extent of interstitial damage and $FSP1^+$ cell number were all significantly higher in non-responders than in responders. Cox regression analysis using two covariates with every possible combination of factors indicated that $FSP1^+$ cell number was the strongest and most significant predictor of corticosteroid responsiveness. When IgAN patients had >32.6 $FSP1^+$ cells/HPF at diagnosis, they were the more likely to show steroid resistance.

Conclusion. $FSP1^+$ cell number can serve as an excellent predictor of corticosteroid responsiveness in patients with IgAN.

Keywords: corticosteroid; FSP1; IgA nephropathy; responsiveness

Introduction

IgA nephropathy (IgAN) is the most commonly occurring glomerulopathy worldwide [1]. IgAN was once thought to be relatively benign and to have a reasonably good long-term prognosis. However, recent studies indicate that 5–25% of IgAN patients progress to end-stage renal disease within 10 years [1–3] and 25–50% do so within 20 years [2]. Prognostic factors for the future development of renal failure include the presence of persistent and severe proteinuria, elevated serum creatinine (Scr) at diagnosis and the presence of hypertension [4–10]. Clinically, proteinuria is the most powerful predictor of poor renal survival, and reduction of proteinuria correlates with improved renal outcome [1–10]. Histologically, renal damage (e.g., crescent formation or severe tubulointerstitial involvement) is the most reliable predictor of an unfavourable renal prognosis [4,6,8,9,11], and two morphometric studies suggest that the extent of tubulointerstitial fibrosis correlates better with reduced renal function than glomerular histology does [12,13].

Recent studies have shown that corticosteroids are an effective treatment for IgAN patients exhibiting a mild reduction of renal function, moderate proteinuria and active histological findings [14–17]; however, there are few published reports describing factors predictive of the response to steroid treatment. According to the Japanese IgAN Treatment Guideline, corticosteroid therapy is recommended for IgAN patients who meet the following criteria: creatinine clearance (Ccr) ≥70 ml/min, daily urinary protein excretion ≥0.5 g/day and active histological lesions on renal biopsy [18]. Nonetheless, recent studies suggest that steroid therapy for IgAN could be beneficial, even when the disease is in an advanced stage [19–21]. We previously reported that renal biopsy specimens from IgAN patients show elevated numbers of $FSP1^+$ fibroblasts, which correlate significantly with the degree of interstitial fibrosis and the deterioration of renal function [22]. The apparent capacity of $FSP1^+$ cell number to serve as a predictive maker of IgAN may make it a useful indicator of the appropriateness of steroid therapy. In the present study, we investigated the

Correspondence and offprint requests to: Masayuki Iwano, 1st Department of Internal Medicine, Nara Medical University, 840 Shijo, Kashihara, Nara 634-8522, Japan. Tel: +81-744-22-3051 (ext. 3411); Fax: +81-744-22-9726; E-mail: miwano@naramed-u.ac.jp

relationship between FSP1$^+$ cell number and responsiveness to corticosteroid therapy.

Materials and methods

Patients

Fifty patients with IgAN (20 males, 30 females) were enrolled in this study after they gave fully informed consent. At the beginning of the study, percutaneous renal biopsies were performed on all patients, and two renal pathologists histologically confirmed the diagnosis of IgAN. Patients with purpura nephritis, lupus erythematosus, diabetes mellitus, neoplasia, viral hepatitis or other infections were excluded. The patients ranged from 14 to 63 years of age (mean 38.2 ± 13.0 years old), and all presented with persistent proteinuria with a baseline that exceeded 2.4 ± 1.8 (0.5–9.6) g/day. Recent studies have described the benefits of steroid therapy for advanced IgAN. We therefore determined the indication for steroid treatment based on the level of proteinuria (≥0.5 g/day) and the presence of active lesions in renal biopsies (cellular/fibrocellular crescents, moderate to severe mesangial proliferation and/or interstitial cell infiltration). The patients were treated with prednisolone at a dose of 30 mg/day for the first 6 months, after which the dose was gradually tapered until it was discontinued at 2 years. In addition, 31 patients received an angiotensin-converting enzyme inhibitor (ACEI) plus an antiplatelet agent during the follow-up, and 38 patients received an angiotensin receptor blocker (ARB) plus an antiplatelet agent.

Clinical and histological parameters

Hypertension was defined as a systolic blood pressure (BP) >140 mmHg and a diastolic pressure >90 mmHg. Urine and blood samples collected at the time of renal biopsy (baseline) were analysed for Scr and 24-h total protein excretion (Up). To measure estimated glomerular filtration rate (eGFR), we selected the modified MDRD equation for Japanese published during the 51st annual meeting of the Japanese Society of Nephrology. Scr was measured every 2 months. At each visit, basic clinical data, including body weight, BP, Scr and Up, were recorded. Renal biopsy specimens that contained at least 10 glomeruli were considered to be adequate for histological analysis and were analysed semiquantitatively based on the following previously described features [23,24]: (i) percentage of glomeruli showing global or segmental sclerosis (%GS); (ii) severity of mesangial cell proliferation (0 = no proliferation to mild proliferation, with three to four mesangial cells per peripheral lobule; 1 = severe segmental proliferation, with more than four mesangial cells per peripheral lobule; 2 = severe global proliferation. Each glomerulus was scored individually, and the mean scores were calculated for all non-sclerosed glomeruli); (iii) percentage of glomeruli showing crescent formation; (iv) percentage of glomeruli showing adhesions; (v) extent of interstitial damage and chronic inflammation (0 = 0–24%, 1 = 25–50%, 2 = >50% of biopsy area showing damage or inflammation); (vi) severity of arteriolosclerosis or arteriolar hyalinosis (0 = no hyalinosis to mild hyaline thickening in at least 1 arteriole; 1 = severe hyaline thickening in at least 1 arteriole; 2 = severe hyaline thickening in many arterioles).

Immunohistochemistry

Renal biopsy specimens were fixed in 10% buffered formalin for 12 h, dehydrated, embedded in paraffin and sectioned according to standard procedures. After deparaffinizing the sections, they were incubated with proteinase K (0.4 mg/ml) for 5 min at room temperature, after which endogenous peroxidase activity was blocked with 0.03% hydrogen peroxide. Nonspecific protein binding was blocked with 5% normal goat serum in PBS containing 2% bovine serum albumin (BSA). The sections were then incubated for 60 min at room temperature with a primary polyclonal anti-FSP1 antibody (1:5000 dilution) [22]. The antibody was then detected using a DAKO Envision+System peroxidase (diaminobenzidine, DAB) kit (DakoCytomation Inc., Carpinteria, CA, USA) and the slides were counterstained with haematoxylin. The specificity of FSP1 staining was confirmed using control rabbit serum and by absorption of the anti-FSP1 antibody using an excess of recombinant FSP1 protein. The numbers of FSP1$^+$ fibroblasts within the cortex were counted in each of 10 random and non-overlapped microscope fields (magnification 200×) and then averaged by two examiners.

Outcome definitions

Patients receiving steroid therapy were divided into two groups based on the changes in their renal function and urinary excretion of protein during the follow-up period. Patients who showed an increase in Scr of <100% from baseline, a reduction in eGFR of <50% from baseline and a decrease in Up of <1.0 g/day were deemed responders (Rs). Patients who showed a total increase in Scr of ≥100%, a total decline in eGFR of ≥50% from baseline or a Up that did not improve to ≤1.0 g/day were deemed to be non-responders (NRs).

Statistical analysis

Statistical calculations were made using the Statview 5.0 and JMP 5.1 software packages. Results were expressed as means ± SD, and the statistical analysis was carried out using non-parametric tests. The Mann–Whitney *U*-test and the Wilcoxon signed-rank test were used for paired and unpaired subjects, respectively. Differences in the parameters between the two groups were analysed using the Friedman and Scheffe's multiple comparison test. Spearman rank correlation analysis was used to assess the correlation between the number of FSP1$^+$ cells and several parameters. Receiver operating characteristic (ROC) curve analysis was used to explore the predictive cut-off value for FSP1$^+$ cell number and %GS during corticosteroid treatment. To assess the prognostic impact of FSP1$^+$ cell number on renal survival, the relationship between covariates and renal survival were evaluated using the Cox proportional hazards model. Values of $P < 0.05$ were considered significant in all analyses.

Table 1. Clinical parameters on diagnosis

	Responder	Non-responder	*P*
Patients	38 (76.0%)	12 (24.0%)	
Age (year/o)	37.5 ± 12.8	40.4 ± 13.8	ns
Gender (M/F)	14/24	6/6	ns
Observation period (year)	7.4 ± 3.0	6.2 ± 2.8	ns
Presence of hypertension	19 (50.0%)	8 (66.7%)	ns
SBP (mmHg)	131 ± 19.3	134 ± 13.1	ns
DBP (mmHg)	79.7 ± 13.0	80.7 ± 12.2	ns
Administration of ACEI/ARB	23 (76.7%)	8 (66.7%)	ns
Administration of antiplatelet agents	29 (76.3%)	9 (75.0%)	ns
Additional administration of immunosuppressives	7 (18.4%)	5 (41.7%)	ns
Urinary excretion of protein for 24 h (g/day)	2.1 ± 1.5	3.3 ± 2.3	ns
Serum creatinine (mg/dl)	1.0 ± 0.4	1.4 ± 0.5	0.0109
Estimated GFR (ml/min/1.73 m^2)	68.8 ± 31.8	43.0 ± 18.0	0.0142
Total protein (g/dl)	6.6 ± 0.8	6.6 ± 0.5	ns
Albumin (g/dl)	3.9 ± 0.5	3.9 ± 0.4	ns
Total cholesterol (mg/dl)	231 ± 84.7	218 ± 39.3	ns
IgA (mg/dl)	324 ± 84.7	340 ± 111	ns

Results

Clinical characteristics of the patients

The mean follow-up period was 7.1 ± 3.0 years. During the follow-up, 38 patients maintained stable renal function, and Up declined to <1.0 g/day. These patients were deemed to be Rs. The remaining 12 patients were classified as NRs. Among the NRs, there were five patients whose renal function was stable, but whose Up continued to be >1.0 g/day. The clinical characteristics of the Rs and NRs at the time of enrolment are shown in Table 1. There were no differences between the two groups with respect to age, gender, incidence of hypertension, administration of ACEI/ARB and antiplatelet agents, administration of additional immunosuppressives, and total serum protein, albumin and IgA levels. On the other hand, Scr at the time of enrolment was significantly higher in the NRs than in Rs (1.4 ± 0.5 versus 1.0 ± 0.4 mg/ml, $P = 0.0109$), and eGFR was significantly lower in the NRs than the Rs (43.0 ± 18.0 versus 68.8 ± 31.8 ml/min, $P = 0.0142$). During follow-up, the Rs showed no significant change in renal function. By contrast, the NRs showed a decline in renal function that was significant by the end of the study (Figure 1). At the time of enrolment, there was no significant difference in Up between the two groups, and Up was significantly lower in both groups after corticosteroid therapy, but the reduction was greater in the Rs (Figure 1). Notably, whereas the Rs showed a significant decline in blood pressure during the follow-up period, the NRs did not (Figure 2). Total serum protein and albumin also significantly increased during the follow-up in the Rs but not in the NRs (Figure 2).

Histological characteristics and steroid responsiveness

The histological features of the two groups at the time of renal biopsy are shown in Table 2. The NRs had significantly more severe mesangial proliferation and interstitial damage than the Rs. percent GS and $FSP1^+$ cell numbers were also significantly higher in NRs. When we then performed ROC curve analyses to determine the predictive cut-off values for %GS and $FSP1^+$ cell number, we found that the cut-offs for corticosteroid responsiveness were 53.5% (sensitivity 0.50, specificity 0.95) and 32.6/HPF (sensitivity 0.75, specificity 0.87), respectively (Figure 3). Moreover, when IgAN patients had >32.6 $FSP1^+$ cells/HPF at the time of diagnosis, they were the more likely to show steroid resistance (Figure 3, Figure 4).

Correlation between the number of $FSP1^+$ cells and the clinical or histological parameters

To clarify the significance of $FSP1^+$ cells during the progression of IgAN, we examined the correlation between various clinical and histological parameters and the numbers of $FSP1^+$ cells (Table 3). Among the clinical parameters examined, $FSP1^+$ cell number was positively correlated with Scr at the time of enrolment [Spearman rank-correlation coefficient (Rs) = 0.552, $P = 0.0003$] and was inversely correlated with eGFR at the time of enrolment (Rs = −0.444, $P = 0.0019$). Among the histological parameters tested, $FSP1^+$ cell number was positively correlated with the %GS (Rs = 0.503, $P = 0.0004$) and the extent of interstitial damage and chronic inflammation (Rs = 0.662, $P < 0.0001$).

Predictive factors for corticosteroid responsiveness

Univariate Cox regression analysis showed that Up, eGFR, the severity of mesangial proliferation, the extent of interstitial damage and chronic inflammation, %GS and $FSP1^+$ cell number all significantly correlated with corticosteroid responsiveness, so their respective risk ratios (RR) were calculated. Estimated GFR [RR 9.63 (95% CI 1.24–74.7, $P = 0.0302$)], the extent of interstitial damage [RR 6.19 (95% CI 1.83–20.9, $P = 0.0033$)], %GS [RR 10.9 (95% CI

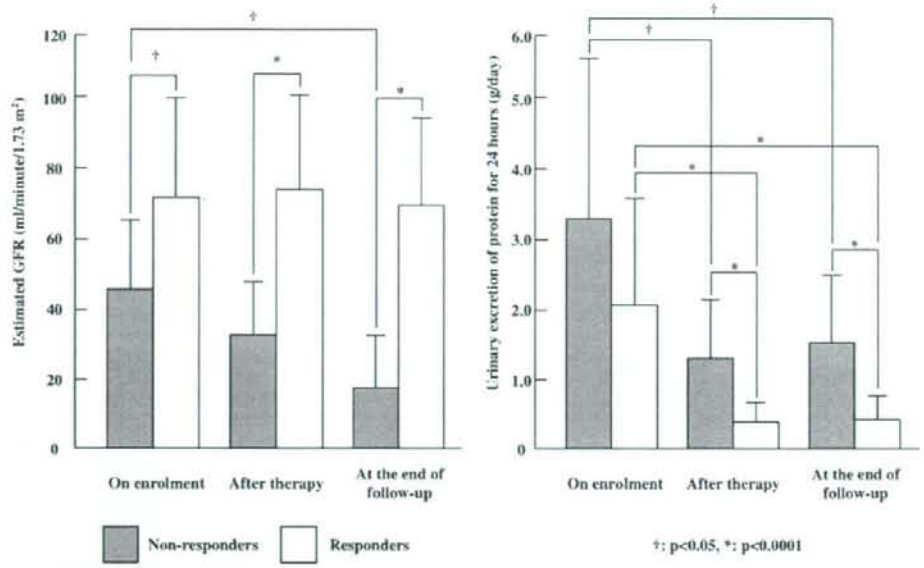

Fig. 1. Changes in Ccr and Up during the follow-up period. During the follow-up period, responders (Rs) showed no significant changes in renal function, whereas non-responders (NRs) showed significantly diminished renal function by the end of the study. At the time of enrolment, there was no significant difference in urinary protein (Up) between the two groups, and Up was significantly reduced in both groups after steroid therapy. At the end of the follow-up, however, the NRs showed significantly higher Up than the Rs.

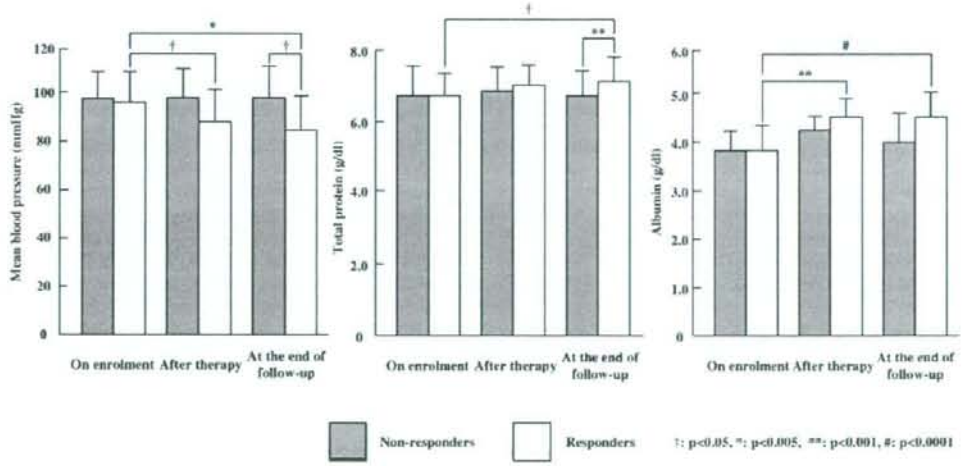

Fig. 2. Changes in mean blood pressure, total protein and albumin during the follow-up period. The responders (Rs) showed a significant decline in blood pressure during the follow-up, but the non-responders (NRs) did not. The Rs also showed significant increases in total protein and albumin during the follow-up, but the NRs did not.

2.69–43.9, $P = 0.0008$)] and FSP1$^+$ cell number [RR 23.5 (95% CI 4.80–115, $P < 0.0001$)] were all significantly predictive of corticosteroid responsiveness (Table 4). Because multiple Cox regression analysis was underpowered in this study, we performed an additional Cox regression analysis using two covariates with every possible combination of factors (FSP1$^+$ cells versus eGFR, interstitial damage and chronic inflammation or %GS) to identify which factor is the strongest predictor. In all analyses, FSP1$^+$ cell number was the strongest and most significant predictor of

Table 2. Histological findings and steroid responsiveness

Histological findings	Responder	Non-responder	*P*
Severity of mesangial proliferation	0.55 ± 0.72	1.25 ± 0.75	0.0072
Percentage of glomeruli showing crescent	13.0 ± 13.4	7.84 ± 8.09	ns
Percentage of glomeruli showing adhesion	9.15 ± 10.9	10.8 ± 10.7	ns
Percentage of glomeruli showing global or segmental sclerosis	20.3 ± 18.9	34.0 ± 24.8	0.0178
Extent of interstitial damage and chronic inflammation	0.947 ± 0.613	1.50 ± 0.798	0.0126
Severity of arteriolosclerosis or arteriolar hyalinosis	0.45 ± 0.60	0.67 ± 0.65	ns
FSP1$^+$ cell	23.0 ± 9.80	35.9 ± 13.1	0.00250

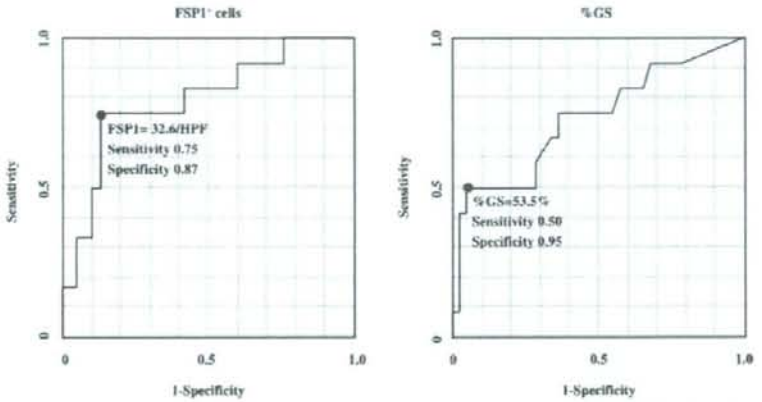

Fig. 3. ROC curve analysis of the association between responsiveness to corticosteroids and FSP1$^+$ cell number and %GS. We performed ROC curve analysis to determine the predictive cut-off values for percentage of glomeruli showing global or segmental sclerosis (%GS) and FSP1$^+$ cell number with respect to responsiveness to corticosteroids. The values obtained were 53.5% and 32.6/HPF for %GS and FSP1$^+$ cell number, respectively.

corticosteroid responsiveness and renal outcome in patients with IgAN.

Side effect of corticosteroid treatment

One patient developed bacterial pneumonia, one patient developed a cataract that required surgery and two patients experienced upper gastrointestinal upset. None of these side effects necessitated discontinuation of treatment.

Discussion

The novel finding of this study is that the FSP1$^+$ cell number at the time of diagnosis is closely associated with responsiveness to corticosteroid therapy and renal outcome in patients with IgAN. Corticosteroids are usually administered to IgAN patients with active histological findings, but an earlier report showed that 30% of those patients do not respond to steroid therapy [16]. Because corticosteroids have many adverse side effects, it would be greatly beneficial if, prior to administration, we were able to identify those patients who will most likely respond to steroid treatment. In addition to conventional clinical and histological parameters, we chose FSP1$^+$ cell number as a possible predictor of steroid responsiveness. FSP1 was first cloned in mice by Strutz *et al.* [25]. Iwano *et al.* then showed that FSP1 is a specific maker of activated fibroblasts and that FSP1$^+$ fibroblasts accumulate in areas of interstitial fibrosis [25,26], which suggests that FSP1$^+$ fibroblasts are the principal effecter cells in renal fibrosis [27].

We previously found that the renal cortices of patients with IgAN contain large numbers of FSP1$^+$ fibroblasts, which correlate closely with the interstitial fibrosis and renal prognosis [22]. Moreover, patients with ≥20 interstitial FSP1$^+$ fibroblasts per HPF had a poor renal outcome. Because tubulointerstitial fibrosis correlates with renal survival [12,13], we decided to evaluate the correlation between the extent of interstitial damage and the responsiveness of IgAN patients to corticosteroid therapy. In the past, the extent of renal fibrosis was studied using computer-assisted morphometric analysis of stained renal biopsy specimens. With this semi-quantitative assay, it takes at least several weeks before the final results are available. This assay is also limited by the degree of methodological variation among examiners. In the present study, we focused on FSP1$^+$ cells, which appear to be a more sensitive and specific marker of both active fibroblasts and renal fibrosis. This approach is simple and quantitative, and the results are available within a few days after renal biopsy (Figure 4a and b).

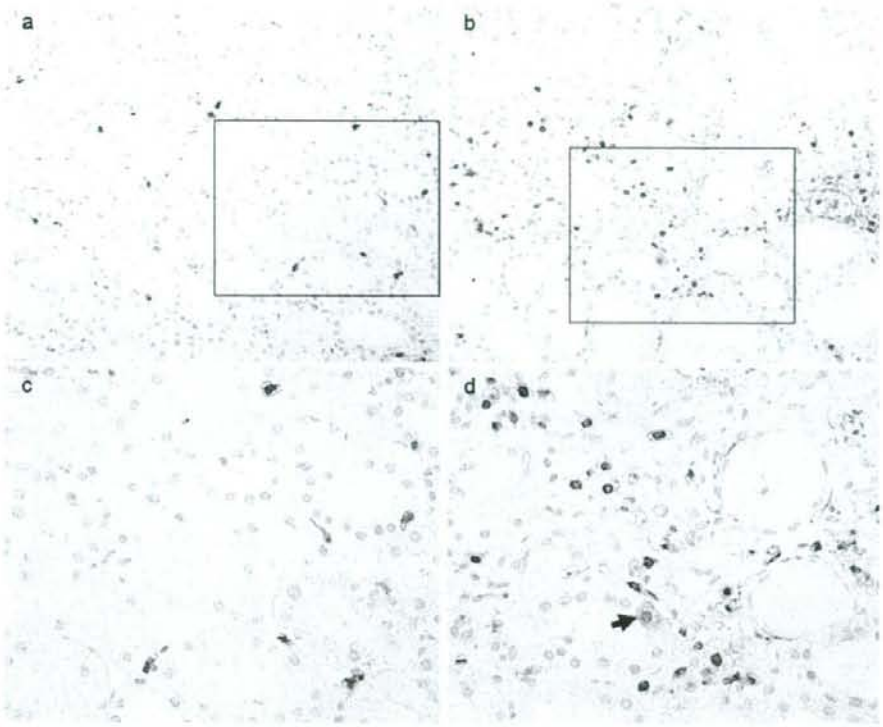

Fig. 4. Representative photomicrograph illustrating FSP1$^+$ expression in the renal interstitium of responders and non-responders. Higher numbers of FSP1$^+$ cells accumulate in the interstitium of non-responder (**b**, **d**) than responder (**a**, **c**). FSP1 was also localized in tubular epithelial cells (arrow). The original magnification in **a** and **b** is 100×; **c** and **d** are the high power images of the boxed areas in **a** and **b**.

Table 3. Correlation of FSP1$^+$ cell number with clinical and histological parameters

Variables	Spearman rank correlation coefficient	*P*
Clinical parameters		
Age	0.160	0.2627
Urinary excretion of protein for 24 h	0.291	0.0419
Serum creatinine	0.552	0.0003
Estimated GFR	−0.444	0.0019
Histological parameters		
Severity of mesangial proliferation	0.141	0.3243
Percent of crescent/total glomeruli	0.267	0.3760
Percent of adhesion/total glomeruli	−0.171	0.5710
Percentage of glomeruli showing global or segmental sclerosis	0.503	0.0004
Extent of interstitial damage and chronic inflammation	0.662	<0.0001
Severity of arteriolosclerosis or arteriolar hyalinosis	0.329	0.0212

We also showed that Scr, eGFR, severity of mesangial proliferation, extent of interstitial damage and chronic inflammation, %GS and FSP1$^+$ cell number were significant predictors of responsiveness to corticosteroids. Interestingly, Cox regression analysis revealed that the number of interstitial FSP1$^+$ fibroblasts was the strongest predictor of corticosteroid responsiveness and renal outcome in patients with IgAN. Moreover, ROC curve analysis showed that the cut-off value is 32.6 FSP1$^+$ cells per HPF. In other words, when IgAN patients have >32.6 FSP1$^+$ cells/HPF, they are much more likely to show steroid resistance.

It is noteworthy that some of the tubular epithelial cells surrounding areas of fibrosis also expressed FSP1, which is consistent with earlier studies describing epithelial–mesenchymal transition (EMT) in regions around areas

Table 4. Univariate Cox regression analysis of predictive factors affecting steroid resistance

Variables	Risk ratio (95%-CI)	*P*
Clinical parameters		
Urinary excretion of protein for 24 h (≥3.0 g/day)	1.72 (0.52–5.72)	0.3791
Estimated GFR (<60 ml/min/1.73 m^2)	9.63 (1.24–74.7)	0.0302
Histological parameters		
Severity of mesangial proliferation (severity sore ≥1)	2.97 (0.64–13.8)	0.1654
Extent of interstitial damage and chronic inflammation (score ≥2)	6.19 (1.83–20.9)	0.0033
%Global or segmental sclerosis (≥50.0%)	10.9 (2.69–43.9)	0.0008
$FSP1^+$ cell (≥32.6/HPF)	23.5 (4.80–115)	<0.0001

of fibrosis [27,28]. Using FSP1 staining as a predictor of steroid responsiveness, we were able to assess not only tissue fibroblasts, but also the emergence of fibroblasts via EMT, which could be indicative of future fibrotic processes. This would make counting $FSP1^+$ cells a more sensitive and specific method than traditional morphometric analysis for evaluating current and future renal fibrosis, and could explain why the statistical power of counting $FSP1^+$ cells is much greater than traditional clinical and histologic parameters for predicting responsiveness to corticosteroids.

In the present study, 24.0% of patients with IgAN did not respond to corticosteroid treatment. That level of responsiveness is compatible with the level reported earlier by Pozzi [16], who found that ~30% of IgAN patients did not respond to steroids. We suggest that $FSP1^+$ cells, including fibroblasts emerging via EMT, represent an ongoing fibrotic process, and the presence of large numbers of $FSP1^+$ cells indicates a need for more intensive therapy, using additional immunosuppressive drugs, from the outset.

Conclusion

Our findings indicate that the renal $FSP1^+$ cell number is a novel marker to guide steroid treatment in IgAN patients. However, further prospective studies will be needed to fully define the role of $FSP1^+$ cells in the treatment strategy for patients with IgAN.

Acknowledgements. This work was supported in part by research grant 19590960 (MI) from the Ministry of Education and Science of Japan and by Grants-in-Aid for the Research Group on Progressive Renal Diseases from the Ministry of Health, Labor and Welfare of Japan. We would like to express our gratitude to Mrs Miyako Sakaida, Mrs Hiromi Ohura and Mrs Fumika Kunda for their excellent technical assistance.

Conflict of interest statement. None declared. The results were presented in 2006 Renal Week held in San Diego, CA, USA.

References

1. D'Amico G. Natural history of idiopathic IgA nephropathy: role of clinical and histological prognostic factors. *Am J Kidney Dis* 2000; 36: 227–237
2. Koyama A, Igarashi M, Kobayashi M and Members and Co-workers of the Research Group on Progressive Renal Disease. Natural history and risk factors for immunoglobulin A nephropathy in Japan. *Am J Kidney Dis* 1997; 29: 526–532
3. Alamartine E, Sabatier JC, Guerin C *et al.* Prognostic factors in mesangial IgA glomerulonephritis: an extensive study with univariate and multivariate analysis. *Am J Kidney Dis* 1991; 18: 12–19
4. Research Group on Progressive Chronic Renal Disease. Nationwide and long-term survey of primary glomerulonephritis in Japan as observed in 1,850 biopsied cases. *Nephron* 1999; 82: 205–213
5. Emancipator S, Gallo G, Lamm M. IgA nephropathy: perspectives on pathogenesis and classification. *Clin Nephrol* 1985; 24: 161–179
6. D'Amico G. Natural history of idiopathic IgA nephropathy: role of clinical and histological prognostic factors. *Am J Kidney Dis* 2000; 36: 227–237
7. Vleming LJ, de Fijter JW, Westendorp RGJ *et al.* Histomorphometric correlates of renal failure in IgA nephropathy. *Clin Nephrol* 1998; 49: 337–344
8. Haas M. Histologic subclassification of IgA nephropathy: a clinicopathologic study of 244 cases. *Am J Kidney Dis* 1997; 29: 829–842
9. Katafuchi R, Oh Y, Hori K *et al.* An important role of glomerular segmental lesions on progression of IgA nephropathy: a multivariate analysis. *Clin Nephrol* 1994; 41: 191–198
10. D'Amico G, Minetti L, Ponticelli C *et al.* Prognostic indicators in idiopathic IgA mesangial nephropathy. *Q J Med* 1986; 59: 363–378
11. Kincaid-Smith P, Nicholls K. Mesangial IgA nephropathy. *Am J Kidney Dis* 1983; 3: 90–102
12. Daniel L, Saingra Y, Giorgi R *et al.* Tubular lesions determine prognosis of IgA nephropathy. *Am J Kidney Dis* 2000; 35: 13–20
13. Bohle A, Strutz F, Muller GA. On the pathogenesis of chronic renal failure in primary glomerulopathies: a view from the interstitium. *Exp Nephrol* 1994; 2: 205–210
14. Kobayashi Y, Hiki Y, Kokubo T *et al.* Steroid therapy during the early stage of progressive IgA nephropathy. A 10-year follow-up study. *Nephron* 1996; 72: 237–242
15. Pozzi C, Bolasco PG, Fogazzi GB *et al.* Corticosteroids in IgA nephropathy: a randomised controlled trial. *Lancet* 1999; 353: 883–887
16. Pozzi C, Andrulli S, Del Vecchio L *et al.* Corticosteroid effectiveness in IgA nephropathy: long-term results of a randomized, controlled trial. *J Am Soc Nephrol* 2004; 15: 157–163
17. Moriyama T, Honda K, Nitta K *et al.* The effectiveness of steroid therapy for patients with advanced IgA nephropathy and impaired renal function. *Clin Exp Nephrol* 2004; 8: 237–242
18. Tomino Y, Sakai H. Special Study Group (IgA Nephropathy) on Progressive Glomerular Disease. Clinical guidelines for immunoglobulin A (IgA) nephropathy in Japan, second version. *Clin Exp Nephrol* 2003; 7: 93–97
19. Tomiyoshi Y, Sakemi T, Ikeda Y *et al.* Cellular crescents and segmental glomerular necrosis in IgA nephropathy are indicative of the beneficial effects of corticosteroid therapy. *Intern Med* 2001; 40: 862–866
20. Tamura S, Ueki K, Ideura H *et al.* Corticosteroid therapy in patients with IgA nephropathy and impaired renal function. *Clin Nephrol* 2001; 55: 192–195

21. Moriyama T, Honda K, Nitta K *et al.* The effectiveness of steroid therapy for patients with advanced IgA nephropathy and impaired renal function. *Clin Exp Nephrol* 2004; 8: 237–242
22. Nishitani Y, Iwano M, Yamaguchi Y *et al.* Fibroblast-specific protein 1 is a specific prognostic marker for renal survival in patients with IgAN. *Kidney Int* 2005; 68: 1078–1085
23. Ballardie FW, Roberts IS. Controlled prospective trial of prednisolone and cytotoxics in progressive IgA nephropathy. *J Am Soc Nephrol* 2002; 13: 142–148
24. Katafuchi R, Oh Y, Hori K *et al.* An important role of glomerular segmental lesions on progression of IgA nephropathy: a multivariate analysis. *Clin Nephrol* 1994; 41: 191–198
25. Strutz F, Okada H, Lo CW *et al.* Identification and characterization of a fibroblast marker: FSP1. *J Cell Biol* 1995; 130: 393–405
26. Iwano M, Fischer A, Okada H *et al.* Conditional abatement of tissue fibrosis using nucleoside analogs to selectively corrupt DNA replication in transgenic fibroblasts. *Mol Ther* 2001; 3: 149–159
27. Iwano M, Neilson EG. Mechanisms of tubulointerstitial fibrosis. *Curr Opin Nephrol Hypertens* 2004; 13: 279–284
28. Iwano M, Plieth D, Danoff TM *et al.* Evidence that fibroblasts derive from epithelium during tissue fibrosis. *J Clin Invest* 2002; 110: 341–350

Received for publication: 14.9.07
Accepted in revised form: 7.4.08

Clin Rheumatol (2008) 27:1063–1066
DOI 10.1007/s10067-008-0885-1

CASE REPORT

A case of autoimmune hepatitis exacerbated by the administration of etanercept in the patient with rheumatoid arthritis

Koji Harada · Yasuhiro Akai · Sachi Koyama · Yasuhide Ikenaka · Yoshihiko Saito

Received: 19 December 2007 / Revised: 13 March 2008 / Accepted: 18 March 2008 / Published online: 18 June 2008

Abstract A 50-year-old woman was admitted for active rheumatoid arthritis (RA). She was found to have RA 1 year prior to this admission. Past history was unremarkable and she had no family history for rheumatic diseases. As nonsteroidal anti-inflammatory drug (NSAID) and methotrexate were not effective, etanercept was started (25 mg, twice a week). Mild elevation of alanine transaminase (ALT) and aspartate transaminase (AST) was found as an outpatient, and it was considered to be NSAID-induced liver injury. Two weeks after the first dose of etanercept, she developed progressive elevation of AST and ALT with right upper quadrant tenderness and hepatomegaly. Etanercept was discontinued and liver biopsy was performed, which demonstrated portal-area-dominant lymphoplasmacytic inflammatory cell infiltration. She was diagnosed as autoimmune hepatitis (AIH). Glucocorticoid was started with normalized liver function and stable joint symptoms. AIH was thought to be acutely aggravated by the administration of etanercept.

Keywords Autoimmune hepatitis · Etanercept · Rheumatoid arthritis

K. Harada · Y. Akai (✉) · S. Koyama · Y. Saito
First Department of Internal Medicine, Nara Medical University, 840 Shijo, Kashihara, Nara 634-8522, Japan
e-mail: yakai@naramed-u.ac.jp

Y. Ikenaka
Third Department of Internal Medicine, Nara Medical University, Nara, Japan

Introduction

Etanercept is a recombinant soluble tumor necrosis factor (TNF) fusion protein, which inhibits biological activity of TNF. Specific therapy-targeting TNF has been offered as an important advance in the treatment of active rheumatoid arthritis (RA) [1]. Although anti-TNF therapy is a powerful therapeutic armamentarium for the patients with RA, various side effects such as autoimmune disorder and infection have been observed [2]. In this report, we describe the first case of autoimmune hepatitis (AIH) exacerbated by the administration of etanercept for rheumatoid arthritis.

Case report

A 50-year-old woman presented to our outpatient clinic in July 2006 for active RA. She has had RA with Sjögren syndrome (SS) since June 2005. She experienced progressive arthralgia and morning stiffness. As nonsteroidal anti-inflammatory drug (NSAID) and methotrexate were not effective, etanercept was started (25 mg, twice a week). She has had mild liver dysfunction (aspartate transaminase/alanine transaminase 45/62 IU/l) since June 2005 and it was considered to be due to NSAID because reduction of NSAID ameliorated liver dysfunction. Two weeks after the first dose of etanercept, she developed right upper quadrant abdominal pain. Physical examination showed tender hepatomegaly. Several proximal interphalangeal and metacarpophalangeal joints were tender and swollen. Laboratory findings were compatible with acute deterioration of liver dysfunction. She was admitted to our hospital. Her past

Table 1 Laboratory findings of 50-year-old patient

Complete blood counts		Blood chemistry		Serology	
Red blood cells	433×10^4 per microliter	Total protein	8.1 g/dl	CRP	0.2 mg/dl
Hemoglobin	10.4 g/dl	Albumin	4.0 g/dl	IgG	2,471 mg/dl
Hematocrit	33.8%	Total cholesterol	168 mg/dl	IgA	328 mg/dl
White blood cells	4,500/μl	Triglyceride	106 mg/dl		
Neutrophils	61.0%	Creatinine	0.7 mg/dl		
Monocytes	7.0%	Blood urea nitrogen	15 mg/dl	CH50	47 U/ml
Lymphocytes	27.0%	Total bilirubin	1.2 mg/dl	C3	142.5 mg/dl
Platelets	31.2×10^4 /μl	Direct bilirubin	0.6 mg/dl	C4	25.1 mg/dl
Erythrocyte sedimentation rate	98 mm/h	AST	237 IU/l	ANA	×1,280 (speckled)
		ALT	300 IU/l	RF	133 IU/l
		LDH	233 IU/l	IgG	137.8 mg/dl
		LAP	135 IU/l	RAPA	×320
		ALP	488 IU/l	ASMA	(−)
		γ-GTP	126 IU/l	AMA	(−)
		ChE	228 IU/l	LKM1	(−)
		Sodium	142 mEq/l	PR3-ANCA	(−)
		Potassium	4.1 mEq/l	MPO-ANCA	(−)
		Chloride	105 mEq/l	HA-IgM	(−)
		Calcium	9.4 mg/dl	HBs-Ag	(−)
		Phosphate	4.9 mg/dl	HCVAb	(−)
				EB-VCA-IgM	(−)
				EBV-VCA-IgG	×320
				EBV-EBNA	×10
				CMV-IgM	(−)
				CMV-IgG	(+)

ANA antinuclear antibody, *RF* rheumatoid factor, *RAPA* rheumatoid arthritis particle agglutination, *ASMA* antismooth muscle antibody, *AMA* antimitochondrial antibody, *LKM1*, antiliver–kidney microsome type 1 antibody

medical history was unremarkable and she had no family history for collagen vascular, rheumatic, or hepatic disease.

On admission, she was afebrile, normotensive (116/72 mmHg) with regular pulse of 78 per minute. She had right upper quadrant tenderness while the remaining physical examination was unremarkable. Laboratory findings were shown in Table 1. She had normocytic anemia and moderately elevated liver enzyme. Viral antigens and antibodies for hepatitis A, B, C, cytomegalovirus, and Epstein–Barr virus were all negative. Antinuclear antibodies were positive at a titer of 1:1,280. Although neither antismooth muscle nor antiliver–kidney microsome type 1 antibody was negative, fluctuating liver dysfunction together with high titer of ANA and elevated serum immunoglobulin G concentration suggested the presence of autoimmune hepatitis. Liver biopsy was performed and light microscopic examination revealed portal-area-dominant lymphoplasmacytic inflammatory cell infiltration (Fig. 1). Diagnosis of definite AIH was made according to the proposed criteria [3]. The patient was treated with oral glucocorticoid with normalized liver function and stable joint symptoms (Fig. 2). She has normal liver enzyme 6 months after discharge.

Discussion

This is the first report that etanercept could be associated with the deterioration of AIH. Etanercept is a recombinant soluble TNF fusion protein, which inhibits the biological activity of TNF. Although anti-TNF therapy is now used in thousands of patients with RA, there are concerns for various side effects such as autoimmune disorders.

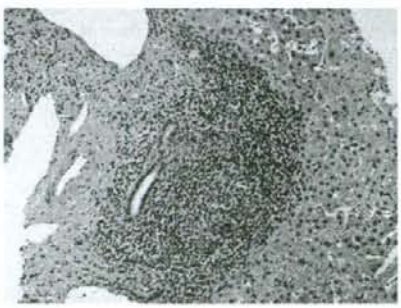

Fig. 1 Light micrograph of liver biopsy. Liver biopsy was performed and light microscopic examination revealed portal-area-dominant lymphoplasmacytic inflammatory cell infiltration

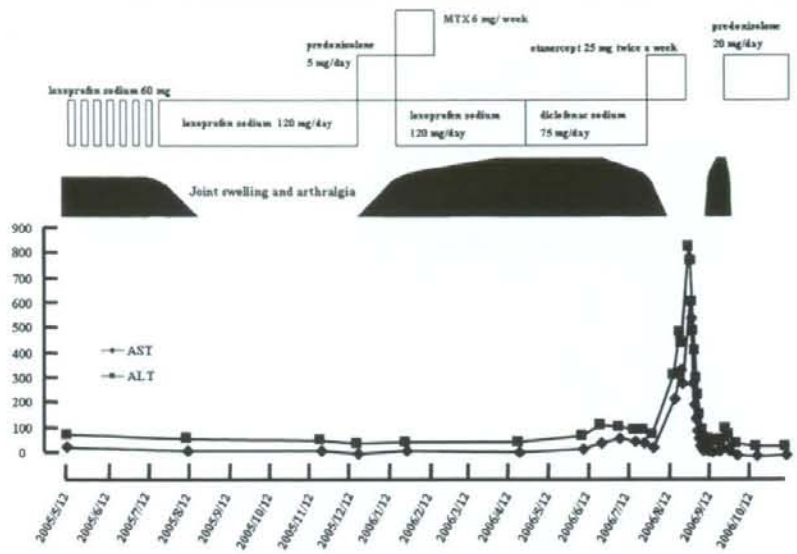

Fig. 2 Clinical course. She has had mild liver dysfunction since June 2005 and it was considered to be due to NSAID. Two weeks after the first dose of etanercept, acute deterioration of liver dysfunction developed

This patient probably had subclinical AIH which was initially considered to be NSAID-induced liver injury. We speculate that clinical course of subclinical AIH was somewhat affected by NSAID and liver function fluctuated according to the dose of NSAID. After etanercept was started, the patient developed clinically apparent liver disease. Clinical course suggested the pivotal role of etanercept in turning AIH to an active state.

We hypothesized that two mechanism might be related to the induction of AIH by etanercept. One hypothesis is as follows: Th1 helper T cell is reported to be associated with the activation of synovitis in RA [4]. Th2 helper T cell, on the other hand, is related to the development of anti-TNF-α-induced autoimmune disease like SLE by activating B lymphocytes [5]. Etanercept acts by inhibiting Th1 helper T cells, thus disrupting the balance between Th1 and Th2 cells [6]. Anti-TNF- α-induced autoimmune disorders could be induced by the imbalance between Th1 and Th2 helper T cells. Liver tissue in the patients with AIH has shown to be infiltrated by more Th2 helper T cells than Th1 cells [7]. By inhibiting Th1 helper cells, etanercept could accentuate the biological action of Th2 cells, which could activate the autoimmune process in the liver. This hypothesis might be further supported by the finding that Th2-mediated cytokine production is increased in AIH patients [7]. Another hypothesis is that etanercept itself could induce AIH. Previous report showed that drug-induced liver injury leads to AIH [8–12]. Drug-induced liver injury could develop AIH by following mechanism which was proposed previously [8]: Drug-induced hepatic cell injury could expose antigens which normally have no contact with immune cells. The exposed antigens would be recognized by immune cells, which could induce liver damage. Etanercept might induce AIH by this mechanism.

In conclusion, caution should be taken for possible association between the use of etanercept and the development of AIH.

Acknowledgment A part of this report was presented in the 51st Annual General Assembly and Scientific Meeting of Japanese College of Rheumatology held in April 2007 in Yokohama, Japan.

Disclosure None

References

1. Olsen NJ, Stein CM (2004) New drugs for rheumatoid arthritis. N Engl J Med 350:2167–2179
2. Roberts L, Mccoll GJ (2004) Tumor necrosis factor inhibitors: risks and benefits in patients with rheumatoid arthritis. Intern Med 34:687–693
3. Johnson PJ, McFarlane IG (1993) Meeting report: International Autoimmune Hepatitis Group. Hepatology 18:998–1005
4. Hartung AD, Bohnert A, Hackstein H et al (2003) Th2-mediated atopic disease protection in Th1-mediated rheumatoid arthritis. Clin Exp Rheumatol 21:481–484
5. Segal R, Dayan M, Zinger H et al (2003) The effect of IL-12 on clinical and laboratory aspects of experimental SLE in young and aging mice. Exp Gerontol 38:661–668
6. Becher B, Blain M, Giacomini PS et al (1999) Inhibition of Th1 polarization by soluble TNF receptor is dependent on antigen-presenting cell-derived IL-12. J Immunol 162:684–688
7. Lohr HF, Schlaak JF, Gerken G et al (1994) Phenotypical analysis and cytokine release of liver-infiltrating and peripheral blood T lymphocytes from patients with chronic hepatitis of different etiology. Liver 14:161–166
8. Krawitt EL (2006) Autoimmune hepatitis. N Engl J Med 354:54–66

9. Schweitzer IL, Peters RL (1974) Acute submassive hepatic necrosis due to methyldopa. A case demonstrating possible initiation of chronic liver disease. Gastroenterology 66:1203–1211
10. Sterling MJ, Kane M, Grace ND (1996) Pemoline-induced autoimmune hepatitis. Am J Gastroenterol 91:2233–2234
11. Gough A, Chapman S, Wagstaff K et al (1996) Minocycline induced autoimmune hepatitis and systemic lupus erythematosus-like syndrome. BMJ 312:169–172
12. Graziadei IW, Obermoser GE, Sepp NT et al (2003) Drug-induced lupus-like syndrome associated with severe autoimmune hepatitis. Lupus 12:409–412

Journal of Thrombosis and Haemostasis, 6: 1352–1359 DOI: 10.1111/j.1538-7836.2008.03022.x

ORIGINAL ARTICLE

Establishment of embryonic stem cells secreting human factor VIII for cell-based treatment of hemophilia A

S. KASUDA*†‡, A. KUBO§, Y. SAKURAI*, S. IRION¶, K. OHASHI**[1], K. TATSUMI*, Y. NAKAJIMA**, Y. SAITO§, K. HATAKE†, S. W. PIPE‡‡, M. SHIMA* and A. YOSHIOKA*

*Department of Paediatrics, Nara Medical University, Kashihara, Nara; †Department of Legal Medicine, Nara Medical University, Kashihara, Nara; ‡Department of Legal Medicine, Hyogo College of Medicine, Nishinomiya, Hyogo; §First Department of Internal Medicine, Nara Medical University, Kashihara, Nara, Japan; ¶Department of Gene and Cell Medicine, Mount Sinai School of Medicine, New York, NY, USA; **Department of Surgery, Nara Medical University, Kashihara, Nara, Japan; and ‡‡Department of Pediatrics, University of Michigan Medical Center, Ann Arbor, MI, USA

To cite this article: Kasuda S, Kubo A, Sakurai Y, Irion S, Ohashi K, Tatsumi K, Nakajima Y, Saito Y, Hatake K, Pipe SW, Shima M, Yoshioka A. Establishment of embryonic stem cells secreting human factor VIII for cell-based treatment of hemophilia A. *J Thromb Haemost* 2008; **6**: 1352–9.

Summary. *Background:* Hemophilia A is an X-chromosome-linked recessive bleeding disorder resulting from an *F8* gene abnormality. Although various gene therapies have been attempted with the aim of eliminating the need for factor VIII replacement therapy, obstacles to their clinical application remain. *Objectives:* We evaluated whether embryonic stem (ES) cells with a tetracycline-inducible system could secrete human FVIII. *Methods and results:* We found that embryoid bodies (EBs) developed under conditions promoting liver differentiation efficiently secreted human FVIII after doxycycline induction. Moreover, use of a B-domain variant *F8* cDNA (226aa/N6) dramatically enhanced FVIII secretion. Sorting based on green fluorescent protein (GFP)–brachyury (Bry) and c-kit revealed that GFP–Bry^+/c-kit^+ cells during EB differentiation with serum contain an endoderm progenitor population. When GFP–Bry^+/c-kit^+ cells were cultured under the liver cell-promoting conditions, these cells secreted FVIII more efficiently than other populations tested. *Conclusion:* Our findings suggest the potential for future development of an effective ES cell-based approach to treating hemophilia A.

Keywords: cell-based therapy, embryonic stem cells, factor VIII, hemophilia A.

Correspondence: Atsushi Kubo, First Department of Internal Medicine, Nara Medical University, 840 Shijo, Kashihara, Nara 634-8522, Japan.
Tel.: +81 744 22 3051 ext. 3411; fax: +81 744 22 9726.
E-mail: akubo@naramed-u.ac.jp

[1]Present address: Institute of Advanced Biomedical Engineering and Science, Tokyo Women's Medical University, Tokyo, Japan

Received 24 October 2007, accepted 25 April 2008

Introduction

Hemophilia A is an X-chromosome-linked recessive bleeding disorder resulting from an inversion or mutation within the *F8* gene, and is the most common of the congenital bleeding disorders [1]. The clinical severity of hemophilia A correlates closely with circulating levels of factor VIII (FVIII) protein. Current standard therapy for hemophilia A patients is replacement therapy with intravenous infusion of plasma-derived or recombinant FVIII concentrates [2]. However, the half-life of infused FVIII is short (10–12 h), and the cost of the frequent infusions necessary to maintain adequate plasma levels of FVIII is extremely high. Consequently, the development of a novel therapy leading to constitutive supply of FVIII is much desired in the next stage of the treatment of hemophilia. For that reason, gene therapy for hemophilia has received a great deal of attention [3]. Constant and sustained FVIII synthesis mediated by gene therapy in patients would obviate the risk of spontaneous bleeding without the need for repeated FVIII infusions. Although the gene therapy approach has shown promise in a mouse model [4], some drawbacks, such as hepatic damage or viral contamination in the non-motile sperm, have been reported [5,6].

As another approach, orthotopic liver transplantation (OLT) has also been attempted for the treatment of hemophilia [7]. Moreover, recent studies have shown that transplantation of hepatocytes [8] or sinusoidal endothelial cells [9] corrects the hemophilia A phenotype in mice, suggesting that cell-based therapy using primary cultured cells may be a useful approach to treating hemophilia. However, a disadvantage of these therapies is that there is a shortage of donors for transplantation or cell isolation.

Given the limitations of all the aforementioned therapies, we evaluated the potential of a cell-based therapy that makes use of embryonic stem (ES) cells as the source of active human FVIII. ES cells retain their totipotential capacity when

maintained on mouse embryonic feeder (MEF) cells and are able to spontaneously differentiate and generate various lineages via the embryoid body (EB) stage. We hypothesized that ES cell-based therapy would have unique characteristics that would enable us to overcome the problems associated with gene therapy or primary cultured cell transplantation. First, ES cells can provide a cell source with unlimited expansion capacity, thereby overcoming the shortage of donors for OLT or primary cultured cell transplantation. Second, hepatic damage or the contamination in the non-motile sperm fraction by viral vectors would be avoided, as there is no virus present.

In this study, to induce the human *F8* gene in ES cells, we used an ES cell line (Ainv18) that enables the inducible expression of the *F8* gene under the control of a tet-inducible promoter [10]. Although Ainv18 ES cells have been used previously for functional analysis of the transcriptional factors HoxB4 and Hex [10,11], we used them for synthesis of a secretable protein. Together, these advantageous features could make ES cell-based therapy an effective approach to the treatment of hemophilia A. Our aim in the present study, therefore, was to establish an ES cell line capable of doxycycline (Dox)-inducible *F8* gene expression and to determine the most suitable differentiation conditions for secretion of FVIII. We show that ES cells can secrete FVIII with antigen and coagulant activity, suggesting that ES cell-based therapy may be a potentially useful approach to treating hemophilia A.

Materials and methods

Growth and differentiation of ES cells

The cDNA construct harboring the full-length human wild-type (WT)-*F8* was described previously [12], as were the B-domain-deleted (BDD)-*F8* and 226aa/N6 cDNAs [13]. Ainv18 ES cells (a kind gift from M. Kyba and G. Q. Daley) were transfected with the WT-*F8*-plox, BDD-*F8*-plox or 226aa/N6-plox targeting plasmids by electroporation, yielding tet-WT-*F8*, tet-BDD-*F8* and tet-226aa/N6 ES cells, after which the transfectants were selected with G418, as described previously [11]. Green fluorescent protein (GFP)–brachyury (Bry) Ainv18 ES cells (S. Irion *et al.*, unpublished data) were established by targeting GFP to the Bry locus in Ainv18 ES cells [14].

ES cells were maintained on MEF cells and were passaged twice on gelatin-coated dishes before EB formation, as previously described [15]. To generate EBs, ES cells were dissociated to a single cell suspension with 0.25% trypsin/EDTA and cultured at various concentrations ($1–8 \times 10^3$ cells mL^{-1}) in 60-mm Petri-grade dishes in serum-containing differentiation medium [Iscoves' modified Dulbecco's medium (IMDM) supplemented with penicillin–streptomycin, 2 mM glutamine (Gibco/BRL, Grand Island, NY, USA), 0.5 mM ascorbic acid (Sigma-Aldrich, St Louis, MO, USA), 0.45 mM monothioglycerol (MTG; Sigma-Aldrich), 15% fetal bovine serum (FBS; Vitromex, Geilenkirchen, Germany), 5% protein-free hybridoma medium (Gibco/BRL) and 200 μg mL^{-1} transferrin (Boehringer Mannheim, Indianapolis, IN, USA)]. Cultures were maintained in a humidified chamber in a 5% CO_2/air mixture at 37 °C.

The experimental protocol is depicted schematically in Fig. 1A. When EBs were cultured in differentiation medium for 6 days, EBs differentiated into the mesodermal lineage, which includes mainly hematopoietic and endothelial cell populations (hematopoietic-like EBs). For liver differentiation, EBs were cultured in differentiation medium for 3 days and then transferred to serum replacement (SR) medium [IMDM supplemented with 15% knockout SR (Gibco/BRL), penicillin–streptomycin, 2 mM glutamine, 0.5 mM ascorbic acid, 0.45 mM MTG] and cultured for an additional 7 days. On day 10, the EBs were harvested and replated in 12-well tissue culture dishes coated with Matrigel (Becton Dickenson, San Jose, CA, USA) in IMDM with 15% FBS and 1 μM dexamethasone (Dex; Sigma-Aldrich), which led to the development of liver-like EBs [15].

Undifferentiated ES cells were passaged twice on gelatin. Hematopoietic-like EBs cultured with serum for 6 days were replated on 12-well culture dishes coated with Matrigel in IMDM with 15% FBS and 1 μM Dex for 2 days. Undifferentiated ES cells, day 8 hematopoietic-like EBs and day 13 liver-like EBs were stimulated with Dox for 2 days before assay. For *in vitro* assay of FVIII, the culture media were replaced with 500 μL of serum-free IMDM medium containing 5 mg mL^{-1} bovine serum albumin (Calbiochem, San Diego, CA, USA) [16] with or without human FVIII-free von Willebrand factor (VWF; Haematologic Technologies, Essex Junction, VT, USA). Twenty-four hours later, the supernatant and cell samples were harvested for determination of FVIII activity (FVIII:C) and FVIII antigen (FVIII:Ag) or protein levels.

Gene expression

For gene-specific reverse transcription polymerase chain reaction (RT-PCR), total RNA was extracted using RNeasy mini-kits and treated with RNase-free DNase (Qiagen, Valencia, CA, USA). One microgram of total RNA was reverse-transcribed into cDNA using a Superscript RT kit (Invitrogen, Carlsbad, CA, USA) with random hexamers. PCR was carried out using Taq polymerase (Takara Bio, Shiga, Japan) in PCR buffer, 2.5 mM $MgCl_2$, and 0.2 mM dNTPs. The primers for human specific *F8* were 5′-AGAGTTCCAAGCCTCCAACA-3′ (sense) and 5′-TAGACCTGGGTTTTCCATCG-3′ (antisense). The cycling protocol entailed one cycle of 94 °C for 5 min, followed by 25–35 cycles of denaturation at 94 °C for 1 min, annealing at 60 °C for 30 s and elongation at 72 °C for 1 min, and a final incubation at 72 °C for 7 min. Oligonucleotides for *Rex1*, *Gata1*, *Albumin1* (*Alb*), *transthyretin* (*Ttr*), *tyrosine aminotransferase* (*Tat*), *α-fetoprotein* (*Afp*), *Foxa2*, *Sox17*, *Cereberus*, *E-cadherin* (*E-cad*), *Hex* and *β-actin* have been previously described [15,17]. Quantitative real-time RT-PCR analysis was performed with an Applied Biosystems Prism 7700 Sequence Detection System using TaqMan® universal PCR master mix according to the manufacturer's specifications (Applied Biosystems, Foster City, CA, USA).

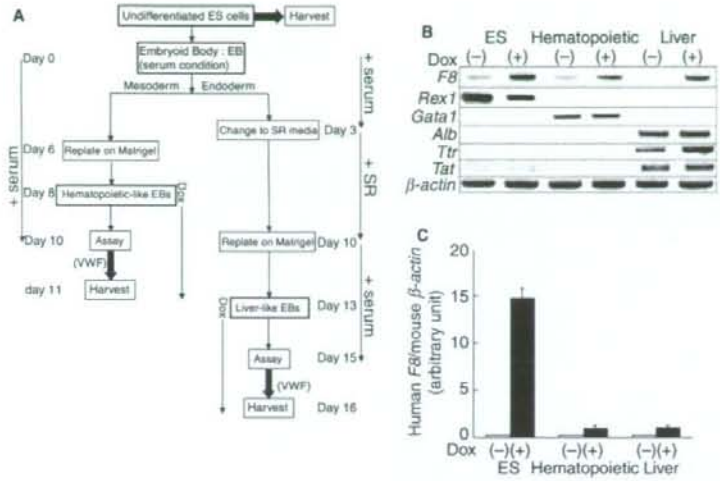

Fig. 1. Expressions of WT-*F8* mRNA by doxycycline (Dox) stimulation in undifferentiated embryonic stem (ES) cells, hematopoietic-like embryoid bodies (EBs) and liver-like EBs. (A) Schema of the experimental protocol. (B) Reverse transcription polymerase chain reaction (RT-PCR) analysis of variable marker genes in undifferentiated tet-WT-*F8* ES cells, hematopoietic-like EBs and liver-like EBs with or without Dox induction (1 μg mL^{-1}). (C) Real-time PCR analysis of *F8* mRNA levels in undifferentiated tet-WT-*F8* ES cells, hematopoietic-like EBs and liver-like EBs with or without Dox induction (1 μg mL^{-1}). The data presented are means of three independent experiments; the error bars represent the SEM. VWF, von Willebrand factor; SR, serum replacement.

The TaqMan probes and primers for human *F8* (assay identification number Hs00240767) and mouse *F8* (assay identification number Mm00433174) were assay-on-demand gene expression products (Applied Biosystems). The mouse *β-actin* gene (assay identification number Mm00607939) was used as an endogenous control.

FVIII assay

FVIII:C was measured in a one-stage activated partial thromboplastin time (APTT) clotting assay in a coagulometer (KC10A; Amelung, Lemgo, Germany) using human FVIII-deficient plasma (George King Biomedical, Overland Park, KS, USA). Activated partial thromboplastin and $CaCl_2$ were purchased from bioMerieux (Durham, NC, USA). FVIII:Ag was quantified using human FVIII-specific enzyme-linked immunosorbent assay (ELISA) kits (FVIII:C-EIA, Affinity Biologicals, Ancaster, ON, Canada), according to the manufacturer's instructions. These ELISA kits employ FVIII light chain specific antibody, and is the same kits used for 226aa/N6 detection previously [13]. For measurement of both FVIII:C and FVIII:Ag, a standard curve was generated using normal human plasma (Coagtrol N; Sysmex, Kobe, Japan) in serial doubling dilutions (1 : 10 to 1 : 1280) in 0.05 M imidazole saline buffer. Each supernatant sample was applied to these assays without dilution rather than 10× dilution. Therefore, FVIII:C and FVIII:Ag levels of culture supernatant samples should be considered as 1/10 of the raw data. We calculated FVIII:Ag levels in normal human plasma as 1 nM. The detection limits of the FVIII:C and FVIII:Ag assays were 10 mIU mL^{-1} and 10 pM, respectively. The attached cell samples in each well were also harvested to determine the amount of protein by a BCA protein assay (Pierce Biotechnology, Rockford, IL, USA). Although these types of data are typically signified in terms of cell number, it is very difficult to count cell numbers in liver-like EBs, due to formation of tight aggregates. In order to adjust secretion levels from the equal protein levels of EBs, FVIII:C and FVIII:Ag levels in the supernatant of each well were adjusted by protein amount of attached cells in the same well. Data are shown as 'not detected' when the raw data for FVIII:C and FVIII:Ag were under the detection limit of the assays (10 mIU mL^{-1} and 10 pM, respectively).

Cell sorting

Day 3.5 EBs were dissociated with trypsin–EDTA, stained with anti-mouse c-kit-phycoerythrin (BD PharMingen, San Diego, CA, USA) in IMDM supplemented with 5% FBS, and sorted in a FACS Aria cell sorter (Becton Dickinson). After sorting, the cells were reaggregated in SR medium and cultured using the liver differentiation protocol.

Results

Tet-WT-F8 ES cells secrete active human FVIII protein

Using the Ainv18 ES cell line, we established ES cells in which the *F8* gene was induced by the tetracycline analog Dox (tet-WT-*F8* ES cells). Tet-WT-*F8* ES cells were cultured such that

we were able to obtain three different cell types: undifferentiated ES cells, enriched hematopoietic EBs (hematopoietic-like EBs), and enriched liver EBs (liver-like EBs). RT-PCR analysis revealed that tet-WT-*F8* ES cells were well differentiated under hematopoietic cell-promoting conditions (hematopoietic conditions) or liver cell-promoting conditions (liver conditions; Fig. 1B), which is consistent with earlier findings [15]. *Rex1* and *Gata1* are marker genes for undifferentiated ES cells and hematopoietic cells, respectively. *Alb*, *Ttr* and *Tat* are marker genes for liver cells. Recently, we further confirmed that liver-like EBs also secreted albumin and transferrin (A. Kubo, unpublished data). Addition of Dox (1 μg mL^{-1}) to the culture medium successfully upregulated *F8* mRNA expression under all three differentiation conditions (Fig. 1B). We also quantitatively analyzed mRNA expression by real-time PCR (Fig. 1C). Interestingly, *F8* mRNA levels in undifferentiated ES cells were much higher than those in hematopoietic-like EBs and liver-like EBs. The reason for this is currently unclear. However, we deduce that gene induction by Dox may be more effective in undifferentiated ES cells than in the other differentiated EBs because of the three-dimensional structure of EBs. On the other hand, *F8* mRNA expression levels of the two cell types were found to be identical. Mouse *F8* mRNA was not induced in liver-like EBs (data not shown). Among the different cell types, FVIII:C and FVIII:Ag were detected only in the supernatant from liver-like EBs; neither was detected with undifferentiated ES cells or hematopoietic-like EBs (Fig. 2A,B). Apparently, the differentiation conditions and the resulting cell types are critical to the production and secretion of FVIII, despite the mRNA levels induced by Dox. In the presence of 2.5 μg mL^{-1} of VWF, Dox-induced levels of both FVIII:C and FVIII:Ag were increased to about twice that seen in the absence of VWF (data not shown). Accordingly, VWF was added at a concentration of 2.5 μg mL^{-1} in subsequent experiments. We also assessed the effect of Dox concentrations on FVIII secretion. When liver-like EBs were stimulated with various concentrations of Dox, the level of *F8* mRNA increased in a dose-dependent manner with increasing

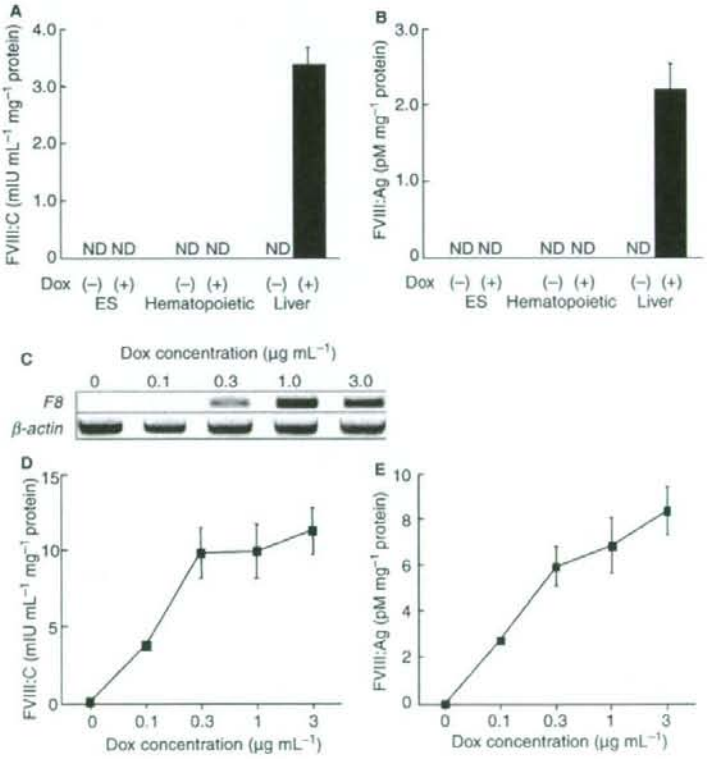

Fig. 2. FVIII:C and FVIII:Ag levels in undifferentiated embryonic stem (ES) cells, hematopoietic-like embryoid bodies (EBs) and liver-like EBs with or without doxycycline (Dox) stimulation. (A, B) FVIII:C (A) and FVIII:Ag (B) levels in media conditioned by cells cultured under the three differentiation conditions, with or without Dox induction (1 μg mL^{-1}). No von Willebrand factor (VWF) was added. (C) *F8* mRNA expression induced by the indicated concentrations of Dox from tet-WT-*F8* ES cells. (D, E) Secretion of FVIII:C (D) and FVIII:Ag (E) from tet-WT-*F8* ES cells induced by the indicated concentrations of Dox in the presence of 2.5 μg mL^{-1} VWF. The data presented are means of three independent experiments; the error bars represent the SEM. ND, not detected.

Dox concentrations (Fig. 2C), and there were corresponding increases in both FVIII:C and FVIII:Ag (Fig. 2D,E).

Tet-226aa/N6 ES cells secrete active FVIII more efficiently than tet-WT-F8 ES cells

Earlier reports showed that BDD-*F8* is more efficient than WT-*F8* for FVIII production, because higher mRNA levels are achieved [18,19]. In addition, Miao *et al.*[13] bioengineered a BDD-*F8* variant with 226 amino acids of the native *F8* B-domain that includes six asparagine-linked glycosylations (226aa/N6). They showed that COS-1 or CHO cells transfected with 226aa/N6 secrete active FVIII more efficiently than WT-*F8*- or BDD-*F8*-expressing cells. To evaluate these three *F8* types with respect to FVIII production and secretion, tet-WT-*F8* ES cells, tet-BDD-*F8* ES cells and tet-226aa/N6 ES cells were cultured under the liver conditions. Real-time PCR analysis showed that BDD-*F8* mRNA was expressed 2-fold higher than WT-*F8*, and 226aa/N6 mRNA levels were between those of WT-*F8* and BDD-*F8* (Fig. 3A). These results suggest that the length of the B-domain may affect the transcriptional levels of the *F8* gene.

FVIII secretion in liver-like EBs from tet-BDD-*F8* ES cells was about 1.5-fold higher than in those from tet-WT-*F8* ES cells (Fig. 3B,C). Furthermore, FVIII secretion in liver-like EBs from tet-226aa/N6 ES cells was about 6–10-fold higher than in those from tet-WT-*F8* ES cells (Fig. 3B,C). These results demonstrated that the construct of 226aa/N6 efficiently produced higher levels of *F8* regardless of transcriptional levels.

Comparison of FVIII secretion in population sorting based on the Bry/c-kit

Recently, Gouon-Evans *et al.* showed that activin can induce definitive endoderm in the absence of serum and that the GFP–Bry$^+$/c-kit$^+$ population was the definitive endoderm progenitor under this condition [20]. We tested whether the GFP–Bry$^+$/c-kit$^+$ population cultured in the presence of serum also contained endoderm progenitors, and which subpopulation gave rise to FVIII-secreting cells. Tet-226aa/N6 ES cells were differentiated for 3.5 days in the presence of serum, at which time the GFP–Bry$^+$ and c-kit$^+$ populations had been induced (Fig. 4A). On the basis of earlier studies [14,20], the GFP–Bry$^+$/c-kit$^-$ and GFP–Bry$^+$/c-kit$^+$ cell fractions were deemed to be mesoderm and endoderm, respectively. After the population was sorted and harvested for RNA isolation, RT-PCR showed that *Foxa2* and *Sox17*, which are normally expressed in endoderm, were expressed primarily in GFP–Bry$^+$/c-kit$^+$ cells (Fig. 4B). *Cereberus* and *E-cad*, which are expressed in ES cell-derived endoderm [17], and *Hex*, which is an important transcriptional factor for liver specification [21], were also strongly expressed in the GFP–Bry$^+$/c-kit$^+$ fraction. Taken together, these results suggest that GFP–Bry$^+$/c-kit$^+$ cells cultured in the presence of serum contained the definitive endoderm population.

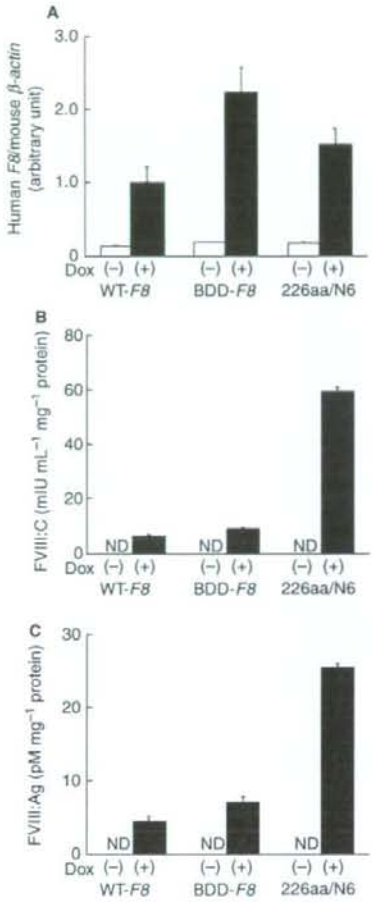

Fig. 3. FVIII secretion from tet-WT-*F8*, tet-BDD-*F8* and tet-226aa/N6 ES cells differentiated under the liver conditions. (A) Real-time PCR analysis of *F8* mRNA levels in tet-WT-*F8*, tet-BDD-*F8* and tet-226aa/N6 ES cells; note that doxycycline (Dox) (1 μg mL^{-1}) induced the highest levels of *F8* mRNA expression in BDD-*F8* cells. (B, C) Secretion of FVIII:C (B) and FVIII:Ag (C) from tet-WT-*F8*, BDD-*F8* and 226aa/N6 ES cells in the presence of 2.5 μg mL^{-1} von Willebrand factor, with or without Dox (1 μg mL^{-1}) induction. The data presented are means of three independent experiments; the error bars represent the SEM. ND, not detected; WT, wild type; BDD, B-domain-deleted.

After sorting, each of the populations derived from tet-226aa/N6 ES cells was reaggregated in SR medium and cultured under the liver conditions. On day 15, EBs derived from GFP–Bry$^+$/c-kit$^+$ cells expressed *Afp* and *Alb* mRNA more strongly than either presorted or GFP–Bry$^+$/c-kit$^-$ cells (Fig. 4C). We then examined the cell populations responsible for the FVIII secretion, and we found that EBs derived from the GFP–Bry$^+$/c-kit$^+$ population were more active for FVIII secretion than the presorted EBs following induction with Dox (Fig. 4D,E). By contrast, GFP–Bry$^-$